

On Free and Forced Barotropic Flows and Their Stability

N.D. Marsh, I.A. Mogensen and A. Wiin-Nielsen

Department of Geophysics, Niels Bohr Institute, University of Copenhagen, Juliane Maries Vej 30, DK-2100 Copenhagen E., Denmark.

(Received: March 1995; Accepted: December 1995)

Abstract

Synoptic investigations have indicated that a sufficiently sharp tropospheric mid-latitude jet stream has the tendency of splitting into two parts, of which one moves north and the other south. This phenomenon has been related to blocking situations. Theoretical investigations suggest that the splitting into a double jet configuration may be explained by a barotropic instability mechanism.

Presented here are the more general results of Wiin-Nielsen's (1961) six component low order model designed to investigate barotropic instability. The model is capable of oscillating between single and double jet states for the unforced, non-viscous case. With the inclusion of Newtonian type forcing, wavelength dependent multiple steady states are possible, the stability of which are influenced by the extent of horizontal shear within the system. For relatively low shear, both a single and double jet configuration are found to be stable, while for extreme shear values only the double jet structure is stable. With extended long term properties of the model for the forced, viscous case, and under certain forcing conditions, such a low order model is capable of capturing the extended barotropic characteristics of double jet blocking situations.

Key words: meteorology, barotropic flows, blocking situations, low-order model, stability analysis

1. Introduction

Upper westerly structures are known to become unstable when the configuration of a single maximum jet stream is sufficiently sharp (Cressman, 1950; Riehl *et al*, 1950). This can result in the splitting of the jet stream into a northern and southern component, a structure that has been observed to be highly stable, often lasting for periods of 1 to 2 weeks occasionally longer (Rex, 1950). Such a development is often referred to as the establishment of a blocking situation, and is an example of internally generated low-frequency variability. Internal instability is normally a result of barotropic shear zones at the smaller scales within a flow. However, evidence suggests that the low frequency behaviour of a spatially stable mean flow may be the result of larger scale barotropic instability (Holton, 1992). Atmospheric energy calculations support this theory revealing that at least two independent regimes exist, typically baroclinic and barotropic. During periods of barotropic instability, the majority of energy is contained at the large-scales, and as such are conducive to the generation of anomalous zonal flows (Wiin-Nielsen, 1986).

Previous studies with forced, simple low order barotropic systems, on the sphere (*Wiin-Nielsen, 1979*), and the β -plane (*Charney and Devore, 1979*), have concluded that barotropic instabilities dependent on the intensity of forcing are capable of producing multiple, stable steady states. In addition, under certain forcing conditions, some of these stable states may contain enough energy on the wave components necessary for double jet configurations.

Wiin-Nielsen (1961) investigated some basic properties of the zonal flow by employing a six-component, barotropic model, without forcing or dissipation. The model included two components to describe the zonal flow, and four components to describe eddies capable of transporting momentum, thus interacting with the zonal components. The instability analysis was performed with a zonal current described by just one of the zonal velocity components, permitting only the nature of a single jet to be investigated. This revealed that for sufficiently large zonal velocities, corresponding to large horizontal shear, a single jet centered on the β -plane channel is unstable.

The purpose of the present paper is to report on investigations of the same six-component model, but with the instability analysis performed using a zonal flow described by both velocity components. In addition, Newtonian forcing and dissipation have been added, allowing the possibility of investigating the stability of multiple steady states.

2. *The low order model description*

The model's geometry is a rectangular region (x, y) , with boundary conditions of periodicity described by the eddies in the east-west direction, and no meridional flow at the southern and northern "walls". The basic state is described by two velocity components for the zonal flow (z_2, z_4) , and four velocity components for the eddies (x_1, y_1, x_3, y_3) . The zonal flow describes the shape of the wind profile across the channel, i.e. N-S direction, which in this model is represented by a constant velocity (z_2+z_4) , and meridional wave components 2 and 4. For a channel width D , and with $\lambda = \frac{\pi}{D}$, the zonal velocity is given as:

$$u_z = z_2(1 - \cos(2\lambda y)) + z_4(1 - \cos(4\lambda y)) \quad (1)$$

The eddies are selected to have meridional wave components 1 and 3, facilitating the so called 'triad' interaction between all components describing the basic state. The model is restricted to a single wave number, $k = \frac{2\pi}{L}$ where L is the zonal wavelength. The width of the channel, D , is kept within allowable limits for a β -plane approximation, and is set to $D = 7.0 \times 10^6$ m for all calculations presented here.

The zonally averaged and eddy streamfunctions are then respectively:

$$\begin{aligned}\Psi_z(y,t) &= D(z_2 + z_4) \left[1 - \frac{y}{D} \right] + \frac{z_2}{2\lambda} \sin(2\lambda y) + \frac{z_4}{4\lambda} \sin(4\lambda y) \\ \Psi_e(x,y,t) &= \frac{x_1}{k} \sin(\lambda y) \sin(kx) + \frac{y_1}{k} \sin(\lambda y) \cos(kx) + \\ &\quad \frac{x_3}{k} \sin(3\lambda y) \sin(kx) + \frac{y_3}{k} \sin(3\lambda y) \cos(kx)\end{aligned}\quad (2)$$

The complete streamfunction is then:

$$\Psi(x,y,t) = \Psi_z(y,t) + \Psi_e(x,y,t) \quad (3)$$

These functions are inserted into the barotropic vorticity equation applied on the β -plane. The orthogonality of trigonometric functions across the channel with length L and width D , reduces the system to six equations describing the development of six velocity amplitudes; $z_2, z_4, x_1, x_3, y_1, y_3$ over time. These equations, with the addition of Newtonian forcing are then (Wiin-Nielsen, 1961):

$$\frac{dz_2}{dt} = 2kQM + \gamma(z_2^* - z_2) \quad (4)$$

$$\frac{dz_4}{dt} = -2kQM + \gamma(z_4^* - z_4)$$

$$\frac{dx_1}{dt} = k[(z_4 - a_1 z_2 - b_1)y_1 - (a_2 z_2 + a_3 z_4)y_3] + \gamma(x_1^* - x_1)$$

$$\frac{dy_1}{dt} = -k[(z_4 - a_1 z_2 - b_1)x_1 - (a_2 z_2 + a_3 z_4)x_3] + \gamma(y_1^* - y_1) \quad (5)$$

$$\frac{dx_3}{dt} = k[(z_2 + z_4 - b_3)y_3 + (a_4 z_2 - a_5 z_4)y_1] + \gamma(x_3^* - x_3)$$

$$\frac{dy_3}{dt} = -k[(z_2 + z_4 - b_3)x_3 + (a_4 z_2 - a_5 z_4)x_1] + \gamma(y_3^* - y_3)$$

where for convenience we have introduced the notation:

$$\begin{aligned}M &= x_1 y_3 - x_3 y_1 & Q &= \frac{\lambda^2}{k^2} & R &= \frac{\beta}{k^2} \\ a_1 &= \frac{Q-3}{2(1+Q)} & a_2 &= \frac{5Q+1}{2(1+Q)} & a_3 &= \frac{7Q-1}{2(1+Q)} \\ a_4 &= \frac{3Q-1}{2(1+9Q)} & a_5 &= \frac{15Q-1}{2(1+9Q)} \\ b_1 &= \frac{R}{(1+Q)} & b_3 &= \frac{R}{(1+9Q)}\end{aligned}\quad (6)$$

The term $\gamma(x^* - x)$, where x represents any one of the six velocity amplitudes, is the Newtonian forcing applied to the system. The rate of forcing is described by γ , the extent of which is given by the forcing parameter x^* of the respective velocity component.

3. *Stability of the unforced zonal current*

Here the stability of an unforced ($\gamma = 0$) zonal flow to small wave perturbations is analysed. The arbitrary zonal current is described by two velocity components, (z_2, z_4) , permitting the stability analysis of both double and single jet structures. Time dependence is assumed to take the exponential form, and the eigenvalues are found by solving the resulting 4×4 matrix using a standard routine.

The quantity z_2+z_4 describes the constant element of the zonal velocity (Eq. 1), and as such is analogous to zonal momentum which is conserved, as seen from the summation of both zonal flow equations (Eq. 4). An estimate of the observed mean zonal wind at 500 mb between equator and pole is between 0-30 m/s (Holton, 1992), this range of values for zonal momentum is used in the following calculations. With these restrictions the critical curve, i.e. transition from stability to instability, can be computed by setting zonal momentum to 15 m/s and finding z_2 as a function of wavelength L (Fig. 1). This enables the selection of an unforced initial state, with well known stability conditions, prior to an experimental run. The solution has an asymptote at $L \simeq 4.8 \times 10^6$ m for both negative roots, apparent from Fig. 1 where the critical curve tends to \pm infinity. As L tends to zero the critical curves for both the lower negative and positive roots converge, reducing the possibility of small scale instabilities. Fig. 1 reveals that unstable regions are restricted to areas between the critical positive root and lower negative root, and also above the upper critical negative root. All other regions can be considered as stable for the unforced model.

Given a conserved momentum, it is possible to determine a single or double jet configuration by selecting the velocity amplitude z_2 alone, and observing the critical inequalities:

$$\text{For a single jet: } z_2 > \frac{4}{5} \times \text{momentum}$$

$$\text{For a double jet: } z_2 < \frac{4}{5} \times \text{momentum}$$

$$\text{For a double jet separated by easterlies: } z_2 < 0$$

Observed double jets are not normally separated by easterlies. The region in Fig. 1 corresponding to perhaps more realistic double jets separated by westerlies, indicates that these structures are stable, except for a limited region at the smaller scales.

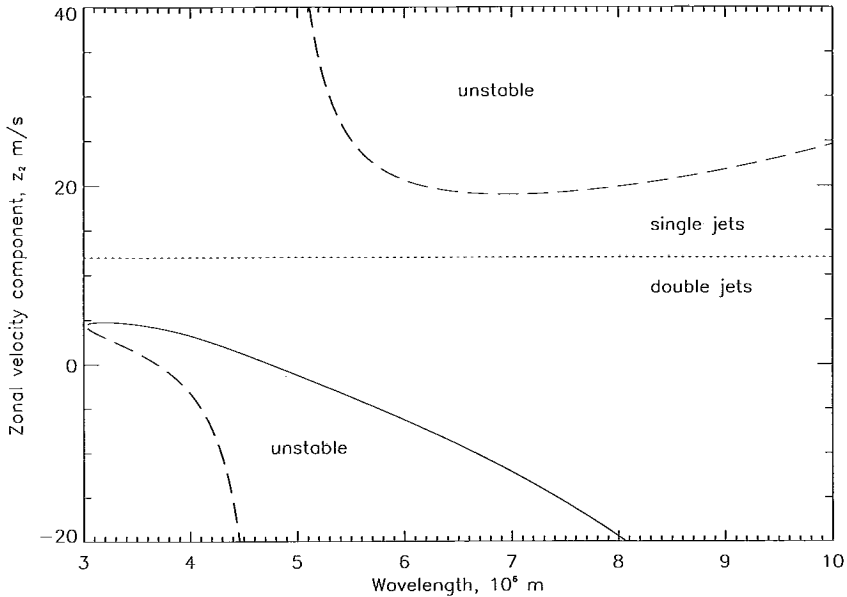


Fig. 1. Stability of the zonal current for the unforced case, including both positive roots (solid line) and negative roots (dashed line). The unstable regions are labelled, all other regions can be considered stable.

To illustrate the performance of this unforced model two integrations are presented, both at a wavelength $L = 7 \times 10^6$ m but with different initial conditions. Fig. 2a displays the zonal velocity behavior in time with initial state $z_2 = 40$ m/s and $z_4 = -15$ m/s when a finite eddy perturbation of $x_1 = 0.001$ m/s is applied. The resulting zonal velocities after approximately 200 hours begin to oscillate in antiphase between their initial values and a minimum (for z_2), maximum (for z_4). The zonal and eddy kinetic energies can also be seen to oscillate in antiphase, as would be expected in an energy conserving environment. The energy conversion (Fig. 2b), reveals how energy is drawn from the zonal flow by the eddies as the wave grows, returning to the zonal flow as the wave decays.

Maximum time variations are possible by setting the constant zonal velocity ($z_2 + z_4$) to zero and the eddy component $x_1 = 15$ m/s. The zonal velocities (Fig. 3a) again oscillate in antiphase, though with increased amplitudes and a period of approximately 150 hours. Zonal kinetic energy is observed to periodically pass through zero, a result of the initial state being one extreme of the oscillation. The energy conversion (Fig. 3b) is again periodic, though more irregular than the previous example as the wave develops.

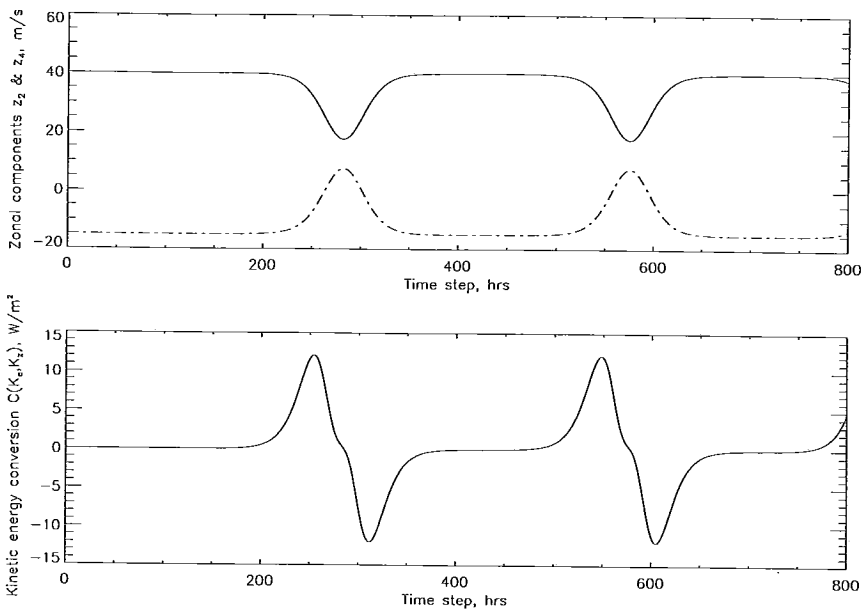


Fig. 2. a) The time variation of velocity components z_2 (solid line) and z_4 (dot dashed line) for an unstable zonal current, with initial values: $z_2 = 40 \text{ m/s}$, $z_4 = -15 \text{ m/s}$ and eddy perturbation $x_1 = 0.001 \text{ m/s}$ b) zonal to eddy kinetic energy conversion.

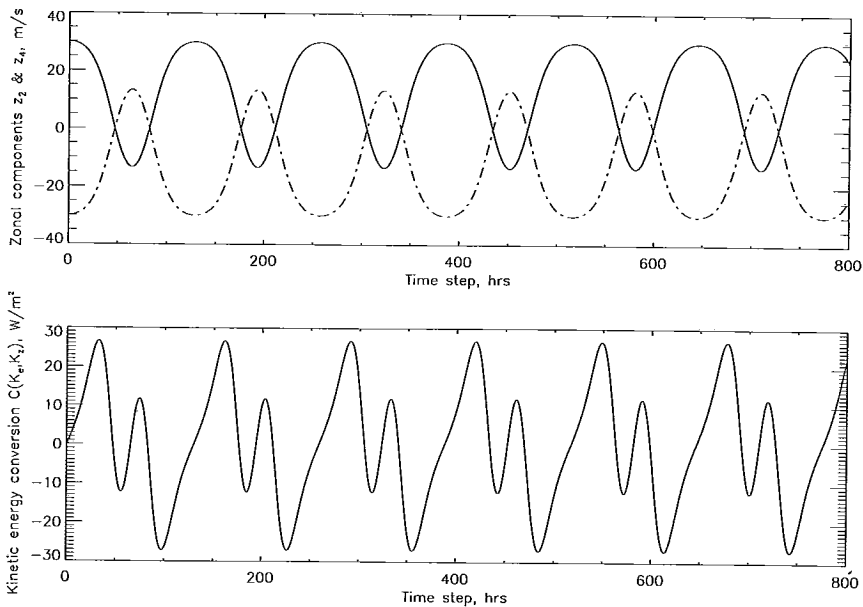


Fig. 3. Cautions as in Fig. 2 with initial values: $z_2 = 15 \text{ m/s}$, $z_4 = -15 \text{ m/s}$ and eddy component $x_1 = 15 \text{ m/s}$

These experiments demonstrate that the model can reproduce the development of a wave as it undergoes a vacillation, and is thus capable of illustrating the essential parts of barotropic development for both single and double jet structures.

4. *Steady states of the forced system*

Constant forcing and dissipation are now added to the system through careful selection of the Newtonian forcing components γ and x^* , providing the possibility of multiple steady states. The four equations for the eddy components (Eq. 5) are linear in x_1 , y_1 , x_3 and y_3 , whose solutions are found and inserted into the equations describing the zonal flow components (Eq. 4). Assuming a steady state, summation of the two zonal equations under stationary conditions reveals the relationship:

$$z_2 + z_4 = z_2^* + z_4^* \quad (7)$$

This permits the elimination of one zonal variable, i.e. z_4 . With the remaining equation now dependent on only z_2 , the real root solutions can be found numerically for given forcing parameters over a range of wavelengths. The stability of the resulting jet structures are then investigated by linearizing the equations around the steady state, and determining the eigenvalues numerically.

In the following experiments the forcing rate was set to a typical value of dissipation in the atmosphere at $\gamma = 1 \times 10^{-6} \text{ s}^{-1}$, eddy forcing parameters were selected to be:

$$\begin{aligned} x_1^* &= 20 \text{ m/s} & x_3^* &= 20 \text{ m/s} \\ y_1^* &= 10 \text{ m/s} & y_3^* &= 10 \text{ m/s} \end{aligned} \quad (8)$$

Fig. 4a displays the solution of zonal velocity z_2 where $z_2^* = 30 \text{ m/s}$ and $z_4^* = 0 \text{ m/s}$, resulting in a single jet maximum of 60 m/s centered on the channel. There is only one stationary, stable solution for the majority of wavelengths up to $L = 8500 \text{ km}$. However, triple solutions are present over a limited interval between 8550 - 8770 km, where steady states with largest and smallest values of z_2 are found to be stable, while the middle state is unstable. For wavelengths larger than this interval only one stable solution is obtained, though with a considerably reduced value of z_2 .

For the majority of sensible values on forcing parameters z_2^* and z_4^* the stability scenario is similar to that above, but the extent and position of the triple solution wavelength interval is forcing parameter dependent. In extreme cases, with a large difference between z_2^* and z_4^* , the stability of triple solutions can differ. Fig. 4b shows a case where $z_2^* = 30 \text{ m/s}$ and $z_4^* = -20 \text{ m/s}$, again regions with a single state are stable, however only the lower z_2 state is stable over the triple solution interval (5000-10000 km). A possible reason for the instability

of the largest z_2 state is that the steady state jet is now extremely sharp with a relatively small wave amplitude. It is understood that the jet would be highly unstable if the perturbation was infinitesimally small, but also small, finite disturbances are found to be unstable.

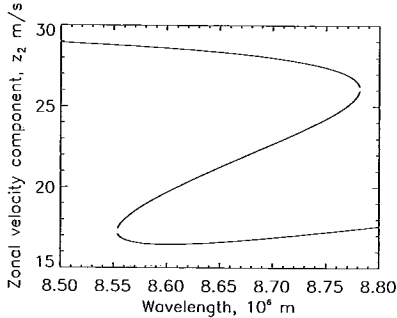


Figure 4a

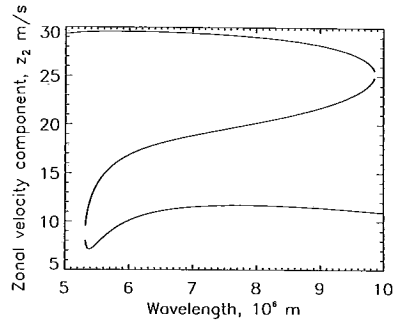


Figure 4b

Fig. 4. Steady states of a forced flow with forcing parameters $x_1^* = x_3^* = 20, y_1^* = y_3^* = 10$, a) $z_2^* = 30, z_4^* = 0$, and b) $z_2^* = 30, z_4^* = -20$.

The number of steady states is wavelength dependent, with the interval extent of multiple solutions determined by forcing parameters. This wavelength dependency is emphasized by differences in the time development of eddy components x_1, y_1, x_3 and y_3 , between single and multiple steady states. Fig. 5a displays the time development of x_1, y_1 (x_3, y_3 identical but not shown) at wavelength $L = 8000$ km, which eventually forms a stable limit cycle. Observing the behavior of these same quantities at wavelength $L = 8100$ km, Fig. 5b reveals that the asymptotic state is now a point in the x_1, y_1 space (x_3, y_3 again identical but not shown), corresponding to one stable state.

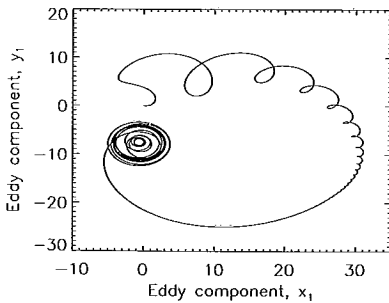


Figure 5a

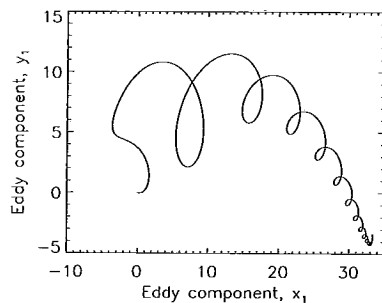


Figure 5b

Fig. 5. Trajectories of the point x_1, y_1 with forcing parameters $z_2^* = 30, z_4^* = -5, x_1^* = x_3^* = 20, y_1^* = y_3^* = -5$, a) $L = 8000$ km, and b) $L = 8100$ km.

For relatively low values of horizontal shear multiple steady states have two stable jet configurations. Those with a high value of zonal velocity z_2 correspond to a sharp single jet. The eddy streamfunction of such a profile (Fig. 6a) is characterized by a low amplitude single maximum centered on the channel. This resembles a high index situation. Lower values of z_2 describe a much broader jet profile on which a high amplitude wave is superimposed producing a double jet structure. The associated eddy streamfunction (Fig. 6b) reveals a high amplitude disturbance divided into northern and southern cells of equal magnitude, reflecting a low index circulation, or blocking. When the horizontal shear within these multiple steady state structures is sufficiently large, only the low index configuration is stable.

These results agree with the quasi-stationary regimes obtained from a much higher resolution, geostrophic, two layer baroclinic model on the β -plane (*Vautard and Legras, 1988*). They found that the cluster of steady state solutions obtained, could be represented by three states; two single jet configurations (zonal), and one double jet configuration (block), all reduced in baroclinicity. Of these three, the block and one zonal solution proved stable. The jet of the zonal solution was maintained almost exclusively by advective terms, while the block persisted largely as a result of transient feedbacks from the small scales to the large scale. This agrees with the present results where multiple steady states are obtained at the larger scales, and that under forcing conditions where only blocking structures are stable, the corresponding region of stability extends over a wide range of the large scales. Although the representation of forcing in the present six component model is too crude to distinguish between the mechanisms maintaining individual stable steady states, it has proved capable of reproducing the main characteristics of large scale features in the zonal flow.

5. Conclusions

These results indicate that the expanded *Wiin-Nielsen* (1961) unforced, non-viscous six component model is capable of producing both single and double jet structures over a range of wavelengths. These can either be stable or unstable, but when considering realistic values of zonal momentum for which double jet structures exist, they are found to be stable for the majority of wavelengths. Time integrations of the model reveal that the essential characteristics of barotropic instability are reproduced as the basic state vacillates between single and double jets.

The addition of Newtonian forcing to the system permits multiple steady states for the positive root solution. These are wavelength dependent, occurring as triplets, over intervals determined by the extent of horizontal shear. The forcing parameters (x^*) influence the shear within the system, where increasing the shear both increases the wavelength interval and influences the stability of solutions for multiple steady states. Regions with only single solutions are always stable single jet structures, while the

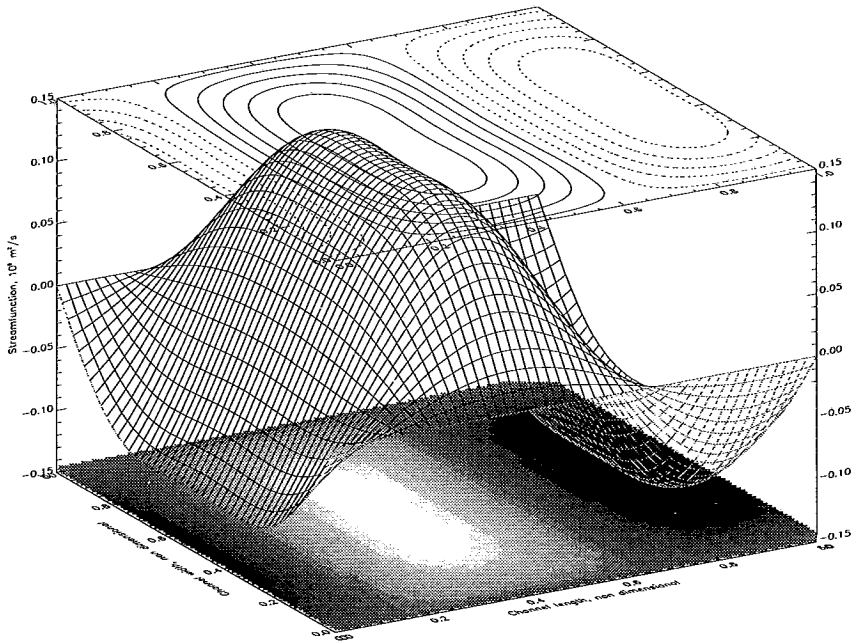


Figure 6a

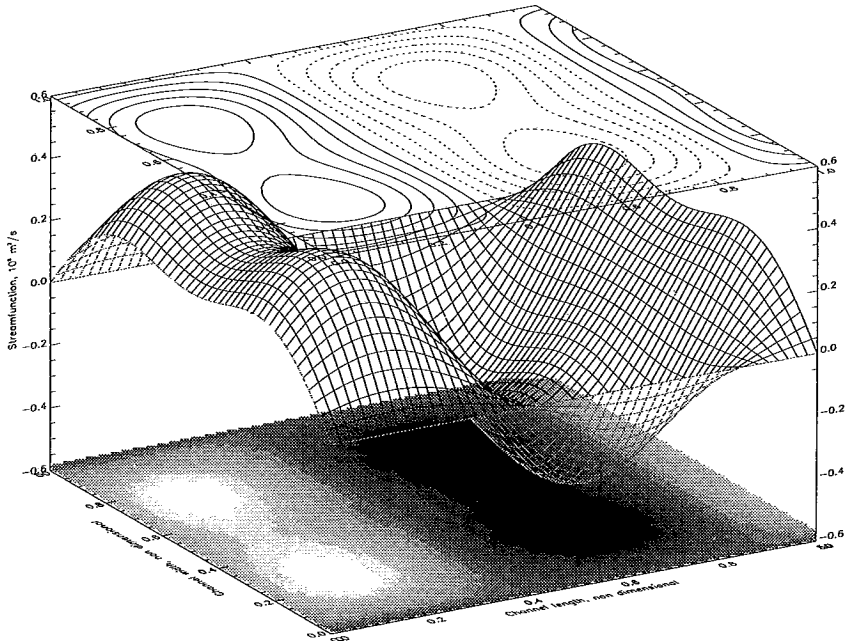


Figure 6b

Fig. 6b. The eddy streamfunctions with forcing parameters as in Fig. 4b a) for a high index case with $z_2 = 28.3 \text{ m/s}$, and b) for a low index case with $z_2 = 16.6 \text{ m/s}$.

multi-solution regions can have either; a stable single and double jet structure concurrently, or one stable double jet structure, depending on the extent of horizontal shear within the flow. In general, the majority of forcing parameters produce stable single jet structures, a large scale feature observed from synoptic analysis of the mid-tropospheric flow. With forcing parameters selected to describe a particularly extreme horizontal shear, only double jet structures are stable, extending over the majority of wavelengths. With the forced systems longer time-scale properties, this low index circulation remains stable for an extended period, which may partly explain why blocking situations persist for so long. The model is thus able to simulate the essential characteristics of a blocking situation, with forcing parameters describing a suitable 'bulk forcing' term.

In its present form, the model is restricted to barotropic conditions, with all forcing and dissipation effects lumped together in one term. Expansion of this term to include descriptions of both boundary layer and internal frictional components, and atmospheric heating, would permit a more physically realistic study of the forcing required to simulate large scale zonal features. A model of this nature will need to be baroclinic, requiring a minimum of 12 components for the inclusion of eddy heat and momentum transports. It is intended that results of such a formulated simple model will follow shortly.

6. References

- Charney, J.G. and J.G. Devore, 1979: Multiple flow equilibria in the atmosphere and blocking. *J. Atmos. Sci.*, **36**, 1205-1216.
- Cressman, G.P., 1950: Variations in the structure of the upper westerlies. *J. Meteor.*, **7**, 39-47.
- Holton, J.R., 1992: An introduction to dynamical meteorology, 3rd edition. Academic Press.
- Rex, D., 1950: Blocking action in the middle troposphere and its effect on regional climate. *Tellus*, **2**, 196-211 & 275-301
- Riehl, H., T.C. Yeh, and N.E. LaSeur, 1950: A study of the variations of the general circulation. *J. Meteor.*, **7**, 181-194.
- Vautard, R. and L. Legras, 1988: On the source of mid-latitude low-frequency variability. Part II: Nonlinear equilibration of weather regimes. *J. Atmos. Sci.*, **45**, 2845-2867
- Wiin-Nielsen, A., 1961: On short- and long-term variations in quasi-barotropic flow. *Mon. Wea. Rev.*, **89**, 461-476.
- Wiin-Nielsen, A., 1979: Steady state and stability properties of a low-order, barotropic system with forcing and dissipation. *Tellus*, **31**, 375-386.
- Wiin-Nielsen, A., 1986: Global scale circulations - A review, in Anomalous atmospheric flow and blocking. *Advances in Geophysics*, **29**, 3-27.